Platelet Responses to Compound Interactions with Thrombin†

Reginald D. Smith‡ and Whyte G. Owen*

Department of Biochemistry and Molecular Biology and Section of Hematology Research, Mayo Clinic and Foundation for Education and Research, Rochester, Minnesota 55905

Received November 19, 1998; Revised Manuscript Received May 18, 1999

ABSTRACT: Catalytic and noncatalytic interactions of thrombin with platelets are investigated with use of thrombin variants with altered specificities and with ligands of thrombin receptors on platelets. Both α-thrombin and weakly coagulant meizothrombin-des-fragment-1 (μ-thrombin) hydrolyze proteolytically activated receptor 1 for thrombin ($rPAR1_T$, recombinant) with catalytic efficiencies of $>10^7$ M^{-1} s^{-1}, whereas $rPAR1_T$ is not a substrate for weakly coagulant β-thrombin. In contrast, both μ-thrombin and β-thrombin are weak agonists of platelet dense body (ATP) secretion. Antibodies that block $rPAR1_T$ cleavage strongly inhibit the secretory reaction to α- and μ-thrombins but not to β-thrombin or to thrombin receptor activating peptide (TRAP). However, catalytically inactive FPR-thrombin, which binds glycoprotein Ib but does not inhibit $rPAR1_T$ cleavage, inhibits responses to TRAP as well as those to α- and μ-thrombins, which indicates that binding of the inactive enzyme to platelets influences the function of $PAR1_T$. An antibody that inhibits binding of thrombin to platelet glycoprotein Ib inhibits secretory responses to thrombin but not to TRAP, so occupancy of glycoprotein Ib per se accounts for only part of the attenuation. All three thrombins stimulate a rise in cytosolic Ca(II), and the dose response to β-thrombin is congruent with that for ATP secretion. However, the response of cytosolic Ca(II) is 10−100 times more sensitive to μ-thrombin and α-thrombin than ATP secretion is, and is inhibited by neither anti-$PAR1_T$ Ig nor FPR-thrombin. Thus, α-thrombin appears to have an activity not shared by either μ- or β-thrombins. This activity is owed to more than coupling of independent signals from cleavage of two proteolytically activated receptors, as there is no synergism when μ-thrombin and β-thrombin costimulate secretion. It is concluded either that α-thrombin has a third interaction site on platelets with which neither μ-thrombin nor β-thrombin interacts or that dual receptors are coordinately cleaved. In either case, the strong secretory response to thrombin appears to be moderated, independently of cytosolic Ca(II), by occupancy of a noncatalytic interaction site such as glycoprotein Ib.

Responses of platelets to thrombin, collectively regarded as platelet "activation", include cytokinesis, aggregation, secretion, and associated metabolic changes. A prerequisite for proteolysis by thrombin for platelet activation has been long established (*1*), inasmuch as mere binding of the enzyme is insufficient to initiate responses (*1*, *2*). A chemical mechanism for proteolysis in platelet activation emerged from cloning of a receptor (*3*, *4*) activated by proteolysis at Arg_{15} to expose a cryptic tethered ligand comprising the first five residues of the new amino terminus.[1] This hitherto unknown mode of receptor activation was established by the capacity of oligopeptides (TRAP,[2] thrombin receptor-activating peptides) bearing the neo-N-terminus to initiate $Ca(II)_C$ flux in transfected *Xenopus* oocytes (*4*). Platelets are distinguished from macrophages and monocytes, where proteolytically inactive thrombin as well as a peptide from the thrombin B-chain sequence are able to elicit chemoattractant and mitogenic responses (*5*−*7*).

There has been, in addition, evidence of multiple distinct proteolytic events for thrombin-induced platelet activation. Studies with mutant (genetic or chemical) thrombins (*8*−*10*), thrombin inhibitors (*11*), and modified platelets (*9*) indicated that changes in thrombin structure or interactive sites can differentially initiate individual platelet responses. Moreover, monoclonal antibodies to the thrombin cleavage site in $PAR1_T$ suppress platelet activation by only the lowest concentrations of thrombin (*12*), TRAP from the rat $PAR1_T$ sequence elicits neither shape change nor aggregation of rat platelets that respond fully to thrombin (*13*), and platelets from mice lacking $PAR1_T$ respond to thrombin and provide hemostasis (*14*). Two additional PAR_Ts, termed PAR3 and PAR4, have now been identified (*15*−*17*). A function for PAR3 in murine platelets has been established directly by dysfunction of platelets from PAR3 knockout mice (*17*) and inhibition with anti-PAR3 Ig (*18*), while functions for PAR4

† Supported by Grant HL47469 from the National Heart Lung and Blood Institute and by the Mayo Foundation.

* To whom correspondence should be addressed. Phone: (507) 284-3776. Fax: (507) 284-8286. E-mail: wgo@mayo.edu.

‡ Present address: Laboratory of Chemical Biology, NIDDK, NIH, Bethesda, MD 20892.

[1] The residue numbering throughout is based on the assumption that the signal peptide is removed during receptor biosynthesis.

[2] Abbreviations: TRAP, thrombin receptor-activating peptide; sTRAP, Ser-{4-fluoro-Phe}-{2-naphthyl-Ala}-Leu-Arg-NH_2; PAR, proteolytically activated receptor; $PAR1_T$, proteolytically activated receptor 1 for thrombin; $rPAR1_T$, recombinant $PAR1_T$; μ-thrombin, meizothrombin-des-fragment 1; FPR-thrombin, thrombin inactivated with $FPRCH_2$-Cl; GP Ib, glycoprotein Ib; $Ca(II)_C$, cytosolic Ca(II); MALDITOF-MS, matrix-assisted laser desorption ionization time-of-flight mass spectrometry; PRP, platelet-rich plasma. The single-letter code for amino acid residues is used throughout.

10.1021/bi9827518 CCC: $18.00
Published on Web 06/17/1999

both in mice (dually with PAR3) and in humans (dually with PAR1) were inferred from the capacity for its TRAP (GYPGKF) to stimulate murine and human platelets (*17*). The ways that these receptors interact to yield specific signals remain unexplored.

Requirements for proteolysis aside, noncatalytic interactions of thrombin with platelets affect responses to catalytic actions. Thrombin binding to platelets has been modeled as a composite of two or three populations of sites, at least one of which is attributed to the platelet membrane glycoprotein Ib (*2*, *19*−*21*). A segment of $PAR1_T$ has been proposed to comprise one of the other sites, but the transience of an enzyme−substrate complex was not addressed (*21*, *22*). Partial suppression of platelet responses to active thrombin by catalytically inactive thrombin (*23*, *24*) or monoclonal antibodies to the thrombin-binding domain of GP Ib (*20*) has been interpreted on one hand as defining GP Ib to be a positive effector of $PAR1_T$-driven activation of platelets or a receptor for α-thrombin capable of activating platelets in its own right (*2*, *19*, *20*, *22*, *23*, *25*), and on the other hand as providing negative regulation of thrombin-induced platelet activation (*26*−*28*). In any case, enzymatically inactive thrombin preparations have never been observed to evoke a metabolic response from platelets.

Thus, the complexities of platelet activation by thrombin include multiple receptors having common responses, common receptors having multiple responses, concurrent irreversible (tethered ligands) and reversible occupancies, tachyphylaxis, paracrine activities, and platelet heterogeneity. Some of the difficulties encountered in interpreting experimental platelet physiology arise from the cooperative cellular reactions that muddle direct and indirect responses. One goal of the investigation presented here is minimization of platelet cooperativity to enhance quantitative analysis of responses to thrombin. Other difficulties arise from the enzymology of thrombin. As a multifunctional, highly regulated enzyme, thrombin has plastic specificity controlled in part by two recognition clefts, termed exosites I and II, that differentially engage macromolecular (i.e., biological) substrates and ligands (*29*). Occupancy of either exosite 1 by thrombomodulin, glycoprotein Ib, or hirudin tail or of exosite 2 by heparin or prothrombin fragment 2 can serve to alter substrate specificity, as do mutations or chemical (including proteolytic) modifications within exosite 1. Among variant thrombins, meizothrombin-des-fragment-1 (*μ*-thrombin), which has exosite 2 occupied by prothrombin fragment 2, and *β*-thrombin, which bears a proteolytic cleavage within exosite 1, share 90−99% reduced activities toward fibrinogen and some other macromolecular substrates in face of full function of their catalytic centers. Because $PAR1_T$ has a sequence centered on $F_{29}WEDEE_{34}$ that is imputed to bind exosite 1 (*30*), *β*-thrombin and *μ*-thrombin provide opportune reagents for investigating the relation between $PAR1_T$ hydrolysis, noncatalytic interactions with thrombin, and platelet responses. This paper describes the use of these thrombin derivatives with altered specificities, of antibodies that block recombinant $PAR1_T$ hydrolysis, and of an approach to platelet assay that eliminates the effects of paracrine and contact-induced platelet activities, in exploring possible interactions among compound receptors that confer strong agonist activity to α-thrombin.

EXPERIMENTAL PROCEDURES

Platelet Dense Body Secretion. Human platelets were obtained from the normal donor pool of the Mayo Clinic Special Coagulation Laboratory. Blood collected in sodium citrate anticoagulant was centrifuged at 200*g* for 8 min, and then 10 *μ*L of the resulting platelet-rich plasma (PRP) was diluted into 800−2000 volumes (to a target of 630 platelets/*μ*L) of sterile Hanks' balanced salt solution (GIBCO) buffered (pH 7.4) with 10 mM Na/HEPES and containing 1 mg/mL bovine albumin and 0.5 g/L glucose (Hanks' medium). Platelet ATP secretion was assayed by bioluminescence using firefly (*Photinus pyralis*) luciferase and luciferin (Boehringer Mannheim) at 30 °C and a final platelet concentration of 250 platelets/*μ*L. Luciferase and luciferin (10 *μ*L) premixed at concentrations of 0.5 mg/mL and 5 mM, respectively, in Hanks' medium were added to 40 *μ*L of dilute platelet suspension and equilibrated for 2 min. Secretion of ATP was initiated by injection of 50 *μ*L of agonist (in Hanks' medium). Luminometry was performed using an apparatus constructed from an SLM spectrofluorimeter photomultiplier tube, to the housing of which was affixed a 3.7 cm × 2.5 cm × 2.5 cm thermostated aluminum block containing the 6 mm × 20 mm glass reaction cuvette 1 cm from the PMT and a rubber septum for the introduction of agonist. Data were acquired for 2−5 min at 1 s intervals as digital files with the OLIS interface and software (OLIS, Inc., Bogart, GA) of the SLM fluorimeter. The response amplitude was standardized by injecting 50 *μ*L of 10 nM ATP, which yielded a peak of 2.9 ± 0.3 V (PMT at 950 kV) within 2 s, and which was used where indicated (Figure 4) to convert volts to ATP units.

Cytosolic Ca(II). The dilute platelets cannot be loaded directly with indo-1 (or any other impermeant dye) because of the irreversibility of uptake and hydrolysis of the AM esters. With the platelet mass being so low, a nontoxic, limiting concentration yields no signal, whereas higher concentrations of dye quickly poison responses. Accordingly, the platelets were loaded in citrate-PRP for 30 min with 1 *μ*M indo-1 AM (Molecular Probes, Inc.), and then diluted with 100 volumes of Hanks' medium. At ca. 5×10^8 platelets/*μ*L (PRP), the indo-1 is limiting and so becomes depleted from the plasma during the loading. With the plasma proteins diluted only 100-fold, addition of tick anticoagulant peptide (a specific prothrombinase inhibitor) blocks thrombin generation that otherwise destabilizes the platelets. After a further 10-fold dilution, these platelets exhibit an ATP secretion dose response to α-thrombin that is indistinguishable from that obtained from direct dilution of the original whole blood 1000-fold. Relative $Ca(II)_C$ is measured in 3 mL cuvettes in an SLM fluorimeter optical bench in a two-channel ratio mode with excitation at 355 nm. The emission, band-pass-filtered at 405 and 455 nm, is collected on-line in separate channels and as the ratio through a DAS-801 A/D eight-channel board and CAC Testpoint acquisition software. This configuration enables on-line screen display of the channels ratio. The routine configuration entails collection at 10 Hz with five-point averaging, for a display rate of 2 Hz. The loaded platelets (2 mL) are placed in the cell holder (30 °C), and after a baseline has been established (ca. 30 s), agonist is added and mixed with use of a plastic rod. All measurements were taken in Hanks' solution [1.2 mM Ca(II)].

Thrombin Variants. α-Thrombin was prepared from porcine blood as described previously (*31*, *32*). Bovine meizothrombin-des-fragment-1 (*μ*-thrombin) was prepared by digestion of bovine prethrombin 1 in 20 mM Tris-buffered saline (pH 8) with partially purified (*33*) *Echis carinatus* venom (100:1 by mass, 5 mM Ca^{2+}) and then by chromatography on QAE-Sephadex with a 0.1 to 0.5 M NaCl gradient in 20 mM Tris-HCl (pH 7.5). Porcine *β*-thrombin was prepared from limit digests of α-thrombin with 1:100 (w/w) trypsin (TPCK-treated, Sigma); after addition of soybean trypsin inhibitor, the *β*-thrombin was purified by chromatography on SP-Sephadex using a 20 to 240 mM sodium phosphate gradient at pH 6 (*34*). Porcine FPR-α-thrombin was prepared by reacting α-thrombin with a 7-fold molar excess of $FPRCH_2Cl$ (Calbiochem), which was removed by SP-Sephadex chromatography in which the bed was washed with 10 column volumes [0.15 M NaCl (pH 6)] before the FPR-thrombin was eluted with 0.6 M NaCl. The absence of residual $FPRCH_2Cl$ was confirmed by diluting the α-thrombin 1:10000 into the FPR-α-thrombin preparation and then measuring residual activity with SpectrozymeTH. The absence of residual thrombin was ensured by treating the FPR-thrombin preparation with 5 mM $^{i}Pr_2$-PF (in which the half-life of thrombin is 0.3 min) for 30 min before it was diluted into Hanks' medium for use, where $[^{i}Pr_2PF] < 10\ \mu M$, too low to interfere with any of the assays. Active enzymes were titrated with *p*-nitrophenyl *p′*-guanidinobenzoate (*35*), and were homogeneous as determined by SDS−PAGE with Coomassie R250 staining. Enzymes were stored as aliquots at −70 °C.

Cloning and Expression of the $PAR1_T$ Extracellular Domain. Construction of a recombinant $PAR1_T$ reagent was based on the assumption that the mature protein lacks its signal peptide which, by homology with plasma proteins in general, ends at P′16 (Ala_{21} in the gene product). The DNA encoding the extracellular domain (residues 1−75, beginning with Arg_{22} of the gene product) of $PAR1_T$ was obtained by PCR from human genomic DNA. All constructs were confirmed by dideoxy sequencing. The clone was expressed as a soluble fusion protein in *Escherichia coli* BL21(DE3)-pLysS using the pET-29(+) vector (Novagen), which carries an N-terminal S·peptide for an expression marker (S·tag assay, Novagen), enterokinase and α-thrombin cleavage sites, and a hexahistidine sequence for affinity purification on Ni^{2+}−Sepharose. Cells were grown at 37 °C on a rotary shaker to an A_{600nm} of 0.6−0.9 and then induced with 1 mM IPTG. The cells were grown for a further 2 h and then harvested by centrifugation for 30 min at 4 °C and 2000*g*. Pelleted cells were lysed in 6 M guanidinium chloride, 20 mM sodium phosphate, and 0.5 M NaCl (pH 7.4), subjected to ultrasonic irradiation (3 × 5 s at 50 mW) on ice, and then clarified by centrifugation (4 °C) at 15000*g*. The clarified lysate was loaded onto a Ni^{2+}−Sepharose column equilibrated with 8 M urea, 20 mM sodium phosphate, and 0.5 M NaCl (pH 7.4). The column was washed with equilibration buffer until $A_{280nm} \leq 0.01$ and then with a similar solvent at pH 6 to the same end point. Bound recombinant was eluted with pH 4 buffer and dialyzed at 4 °C into Tris-buffered saline solution (pH 8) and stored in aliquots at −70 °C, or into water, lyophilized, and stored desiccated at 4 °C. The homogeneity was measured by SDS−PAGE, reversed phase HPLC, capillary zone electrophoresis, and N-terminal sequencing. The molecular mass was determined by MALDITOF-MS. Cleavage products after treatment with α-thrombin were identified by reversed phase HPLC-MALDITOF-MS and N-terminal sequencing. The recombinant protein was radioiodinated with $Na^{125}I$ (Amersham) and chloramine T for 45 s at room temperature, quenched with sodium metabisulfite, and desalted on Sephadex G-25.

$rPAR1_T$ Enzymology. Proteolysis of $[^{125}I]rPAR1_T$ was assessed by densitometry of SDS−PAGE radioautographs. Images of radioautographs were acquired with an HP ScanJet 4C driven with Ofoto 2.0.1 (Light Source Computer Images) in eight-bit grayscale mode and saved raw (TIFF). The image files were opened with NIH Image 1.57; backgrounds were subtracted automatically with the two-dimensional rolling ball method, and numerical density histograms of lanes were acquired within fixed-dimension rectangles encompassing entire lanes. The scanner response, calibrated with a Kodak Control Scale T-14 optical density calibration strip, was linear below 220/255 levels of grayscale, and exposures were limited so that the darkest pixels were less than 200 levels. The progress of rPART hydrolysis was calculated as the quotient of the integral of the rPART band and that of the entire lane. The pseudo-first-order rate constants (k') were extracted from the rPART decay curves by three-parameter nonlinear least-squares fits (SigmaPlot 4, SPSS Software) to a first-order exponential (single exponential with an offset); observed second-order rate constants k'' were calculated as k'/[enzyme].

The K_M of $rPAR1_T$ was measured as the K_i with SpectrozymeTH as the reporter substrate (*36*). Dixon plots were acquired with SpectrozymeTH at K_M, $2K_M$, and $4K_M$ for its respective enzyme (2 *μ*M for porcine α-thrombin, 1 *μ*M for porcine *β*-thrombin, and 4 *μ*M for bovine *μ*-thrombin).

Antibodies. Polyclonal antisera were raised in hens at Panigen, Inc., by immunization with $rPAR1_T$. Immunoglobulins were prepared from yolk (IgY) by poly(ethylene glycol) precipitation (*37*) and from serum (IgG) by triple precipitation in 40%-saturated ammonium sulfate. Anti-$rPAR1_T$ IgY was purified on $rPAR1_T$−Sepharose prepared by reacting $rPAR1_T$ with Affigel-15 (Bio-Rad) in dimethyl sulfoxide. Monoclonal IgG LJ-Ib10, directed against the thrombin-binding epitope on GP Ib (*20*), was provided by Z. Ruggeri; monoclonal IgG SPAN12, directed against the thrombin cleavage site of $PAR1_T$ (*38*), was provided by L. Brass.

Other Materials. The peptide Ser-{4-fluoro-Phe}-{2-naphthyl-Ala}-Leu-Arg-NH_2 (*39*), here abbreviated sTRAP, was synthesized with an Applied Biosystems solid phase synthesizer and purified by C18 HPLC. Equine tendon collagen was obtained from Helena Diagnostics. The thrombin substrate SpectrozymeTH was acquired from American Diagnostica.

RESULTS

Characterization of $rPAR1_T$(1−75). The Ni(II)−Sepharose-purified recombinant fusion protein (Figure 1 header) was >98% homogeneous as determined by reversed phase HPLC (Figure 1A) and had the expected mass as determined by MALDITOF-MS of 15.5 kDa (inset i), while SDS−PAGE

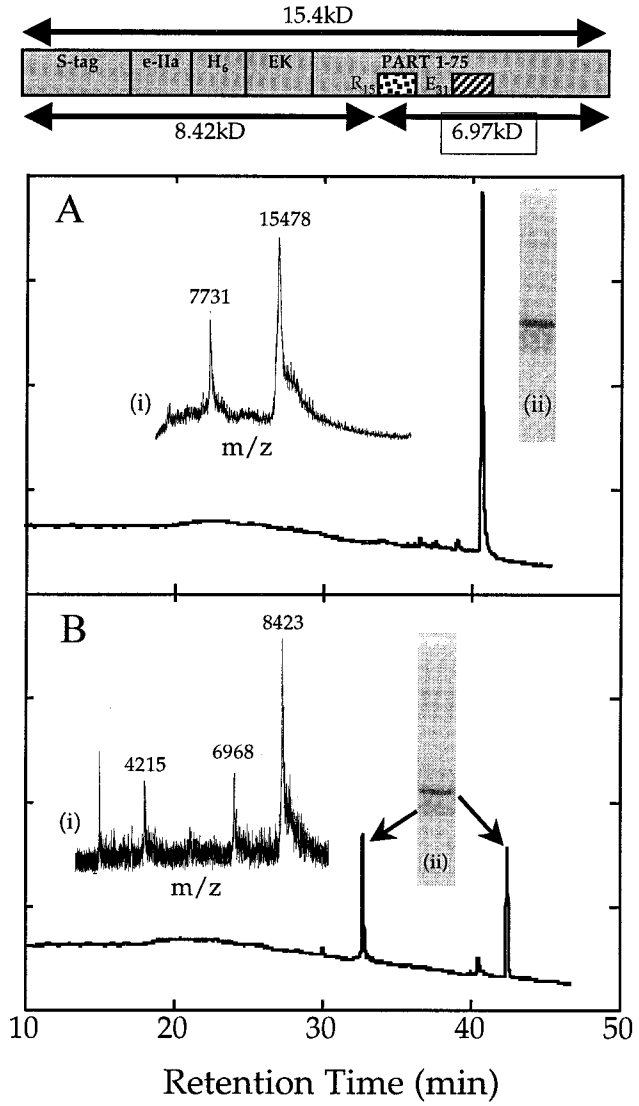

FIGURE 1: Characterization of the chimerical $rPAR1_T$ extracellular domain. (A) Elution of the purified $rPAR1_T$ fusion protein from a C18 HPLC column using an acetonitrile gradient. The insets show MALDITOF-MS analyses (i) and Coomassie-blue-stained 16.5% Tris-tricine SDS−PAGE results (ii). The *m/z* peak at 7731 represents the M^{2+} ion. (B) Digest of $rPAR1_T$ (10 nM α-thrombin, 60 s) analyzed by C18 HPLC, MALDITOF-MS (i), and SDS−PAGE (ii); the peak at 4215 represents the M^{2+} ion of the N-terminal proteolytic fragment. The header illustrates the segments of the fusion protein, including the engineered thrombin cleavage site (eIIa), the polyhistidine (H_6), the engineered enterokinase site (EK), TRAP (stippled box), and the acidic sequence proposed to bind exosite 1 of α-thrombin (hatched box).

(inset ii) showed minor components that by densitometry accounted for 2% of the staining. Treating the recombinant protein with 10 nM α-thrombin for 1 min yielded two products (Figure 1B) with masses expected from cleavage at R_{15} (panel B insets). The identities of the peak at 32 min as the C-terminal 6.97 kDa product ($PAR1_T$ residues 16−75) and that of the peak at 42 min as the N-terminal 8.42 kDa product (ending with $PAR1_T$ residues 1−15) were confirmed by N-terminal sequencing and MALDITOF-MS after HPLC purification. The last methionyl residue in $rPAR1_T$ is at position −1. Accordingly, cleavage of the fusion protein with CNBr (200-fold molar excess) yielded $PAR1_T$(1−75) with the expected mass (MALDITOF) of 8.65 kDa; treatment with 10 nM α-thrombin for 1 min yielded, quantitatively, the 15-residue activation peptide (1.71 kDa) and C-terminal residues 16−75 (6.97 kDa).

Specificity of rPAR1$_T$ as a Thrombin Substrate. Both α-thrombin and μ-thrombin hydrolyze $rPAR1_T$ with catalytic efficiencies comparable to or exceeding the highest known value (*40*, *41*) for substrates of α-thrombin, whereas β-thrombin hydrolyzes the substrate much less efficiently (Figure 2). To ensure the pseudo-first-order constraint that $[S] \ll K_M$, $rPAR1_T$ was radioiodinated and used at concentrations below 50 pM. The $[^{125}I]rPAR1_T$ preparation yielded the products observed in the insets in Figure 1 along with variable amounts of background and side reactions, most prominent with β-thrombin (Figure 2C). Observed second-order rate constants (k''), for hydrolysis of $rPAR1_T$ by α-thrombin, μ-thrombin, and β-thrombin, were calculated from the quotients of measured pseudo-first-order rate constants (k') and enzyme concentrations (Figure 2D). With porcine α-thrombin at a concentration of 1 nM, $[^{125}I]rPAR1_T$ was consumed with a k' of 0.027 s^{-1}, to yield a k'' of 2.7×10^7 M^{-1} s^{-1} (Figure 2A,D). Bovine μ-thrombin, which has a low (10%) clotting specific activity, hydrolyzes $rPAR1_T$ with a k'' of 1.4×10^7 M^{-1} s^{-1}, or 52% of that of porcine α-thrombin (Figure 2B,D). In contrast, $rPAR1_T$ is a minimal substrate ($k'' < 4 \times 10^4$ M^{-1} s^{-1}) for porcine β-thrombin (Figure 2C,D), which also has a low (<1%) clotting specific activity. The engineered thrombin cleavage site (R_{-37}), added to the fusion leader by the manufacturer, is hydrolyzed slowly by all three thrombins, but is most apparent in Figure 2C where the rate at R_{15} is comparable. The progress of cleavage of $PAR1_T$(1−75) analyzed in the same manner (not shown) indicates that the presence of the fusion leader (residues −65 to −1), which enhances visualization by electrophoresis, has no impact on cleavage kinetics by any of the three enzymes.

Cleavage at R_{15} is blocked by both polyclonal and monoclonal anti-$PAR1_T$ Ig (Figure 2, right panels). Specific for the $PAR1_T$ cleavage site, the MoAb SPAN12 allows slow hydrolysis at R_{-37} (Figure 2A), whereas the polyclonal Ig against the fusion protein does not. In contrast, addition of FPR-α-thrombin, catalytically inactive but competent to bind $F_{30}WEDEE_{35}$ and related peptides, has no impact on $rPAR1_T$ hydrolysis by any of the thrombin variants.

The relative catalytic efficiencies of 1, 0.5, and 0.001 (α, μ, and β, respectively) reflect differences in K_M, as measured by competition for a reporter substrate. The K_M of $rPAR1_T$ for α-thrombin was determined (Dixon plot) to be 4 μM, and the K_M for μ-thrombin was found to be 16 μM. For β-thrombin, Dixon plot intercepts ranged between 100 and 200 μM, but proved to be too high for reliable measurement with attainable $rPAR1_T$ concentrations.

Ultradilute Platelet Culture and Quantitative Assay of ATP Secretion. Quantitative analysis of platelet responses to thrombin derivatives and other agonists exacts an assay that reflects direct responses without interference from paracrine activities and physical interactions between platelets. A less obvious pitfall is the free thrombin concentration; platelets, in addition to providing substrate, bind α-thrombin nonproteolytically and with sufficient affinity to sequester a significant portion from solution when platelets are suspended in conventional assay concentrations ($\cong 3 \times 10^5$ μL^{-1}). To address both exigencies, platelets were assayed in short-term, ultradilute culture (250 μL^{-1}), where paracrine activities, interplatelet contact, and α-thrombin binding sites

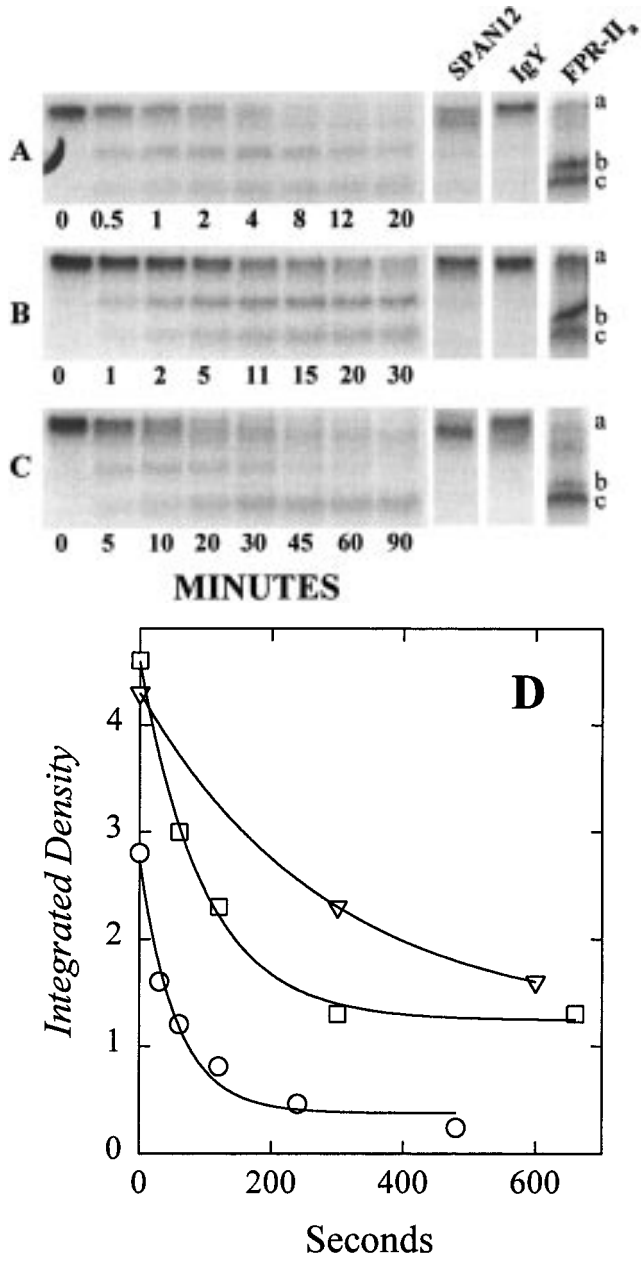

FIGURE 2: Time course of rPAR1$_T$ hydrolysis by thrombin variants. [^{125}I]rPAR1$_T$ was treated with 1 nM α-thrombin (A), 1 nM μ-thrombin (B), and 10 nM β-thrombin (C) in Hanks' medium. At the indicated intervals, samples were quenched with an equal volume of reducing SDS−PAGE sample buffer and then analyzed on 16.5% Tris-tricine gels (*58*). Progress curves were analyzed by densitometry of the radioautographs. Panel D shows three-parameter single-exponential fits (solid lines) of the consumption of rPAR1$_T$ catalyzed by α-thrombin (○), μ-thrombin (□), and β-thrombin (▽). To the right of the progress curve radioautographs are lanes showing the effect of 100 nM SPAN12 MoAb, 200 nM polyclonal IgY, and 100 nM FPR-α-thrombin on hydrolysis of [^{125}I]rPAR1$_T$ (band a) with 1 nM α-thrombin (5 min), 1 nM μ-thrombin (8 min), and 10 nM β-thrombin (45 min). The wider spacing of the N-terminal (band b) and C-terminal (band c) products in the progress curves reflects a recurring variability among radioprotein preparations and may reflect iodination efficiency; the preparation in the right three lanes had $^1/_4$ of the specific radioactivity of the preparation used for the progress curves.

(and plasma proteins) should be diluted to extinction. The α-thrombin dose response of ATP secretion from platelets in ultradilute suspension is shown in Figure 3A. Secretion begins without lag. Comparison with the burst and decay after injection of 10 nM ATP indicates that at all concentrations, including 2.4 μM, some secretion continues for at least 2 min after agonist injection, and for lower concentrations may continue for more than 10 min (not shown). The yield of secreted ATP, obtained by integrating the first derivative of the 10 min progress curve after correction for decay of the oxyluciferin intermediate (0.1 min^{-1}), approaches its maximum by 2−5 nM α-thrombin. The earliest constant secretion rate is used throughout as the rate response to a dose (Figure 3B). A clear maximum rate has not been observed with human platelets and porcine α-thrombin (shown) or human α-thrombin (not shown). The ATP yields were maximal within 20 times the threshold (cf. Figure 4) for all thrombin variants and for sTRAP (Figure 3C). The assumptions that the responses are not influenced by α-thrombin sequestration and paracrine activities are verified in Figure 3D, which shows that the secretion response per platelet is independent of platelet concentration.

Soluble collagen does not directly affect Ca(II)$_C$, which is sensitive to thromboxane A2 (*42*). In keeping with the argument that thromboxane A2 is not a paracrine effector in the dilute suspensions, we confirmed (not shown) that with platelets suspended at 10^4 μL^{-1}, equine tendon collagen in concentrations that induce rapid and maximal ATP secretion had no impact on Ca(II)$_C$.

Responses to Thrombin Variants and the Impact of Anti-rPAR1$_T$ Ig. The extent to which PAR1$_T$ hydrolysis accounts for platelet activation by thrombin should be reflected in principle by the specific activities of thrombin variants in stimulating platelet responses relative to those for PAR1$_T$ hydrolysis. Viewed as the offset either in thresholds or in apparent first inflections (Figure 4), the relative activities are approximately 1, 0.1, and 0.02 (α, β, and μ, respectively). This comparison may overestimate the difference in β- and μ-thrombins, which appear to be nearly overlaid when viewed over larger dose ranges. Affinity-purified chicken anti-rPAR1$_T$ (70 nM) effected a 20-fold (threshold basis) to 100-fold (response offset) suppression of the response to α-thrombin (Figure 4A). The response to μ-thrombin (Figure 4B) is likewise offset by 20-fold, but the response to β-thrombin (Figure 4C) was unaffected. Quantitatively similar offsets (not shown) were obtained with the monoclonal Ig SPAN12 (which binds PAR1$_T$ cleavage site). Higher concentrations of IgY (Figure 4D) and SPAN12 (not shown) partially inhibited β-thrombin as well, but inhibition of all proteases in concentrations at the upper end of their dose responses remained incomplete, while sTRAP-induced secretion was not inhibited (Figure 4D). With both the IgY and SPAN12 antibodies, β-thrombin is inhibited by 40−60%, the distinct value being dependent on the individual platelet preparation but independent of β-thrombin concentration. In all cases, the maximum rates attained with β- and μ-thrombins lie below the maxima attained with anti-rPAR1$_T$-blocked α-thrombin (Figure 4A).

The α-thrombin dose response of the rise in Ca(II)$_C$ lies nearly 2 log units to the left of that of ATP secretion (Figure 5A, upper group). Neither the magnitude nor the shape of the fluorescence signal changes above 100−200 pM α-thrombin, the threshold for dense body secretion. The responses of Ca(II)$_C$ to μ-thrombin (Figure 5A, middle group) reach equivalency with those α-thrombin, but the dose response is right-shifted in proportion to that of dense body secretion.

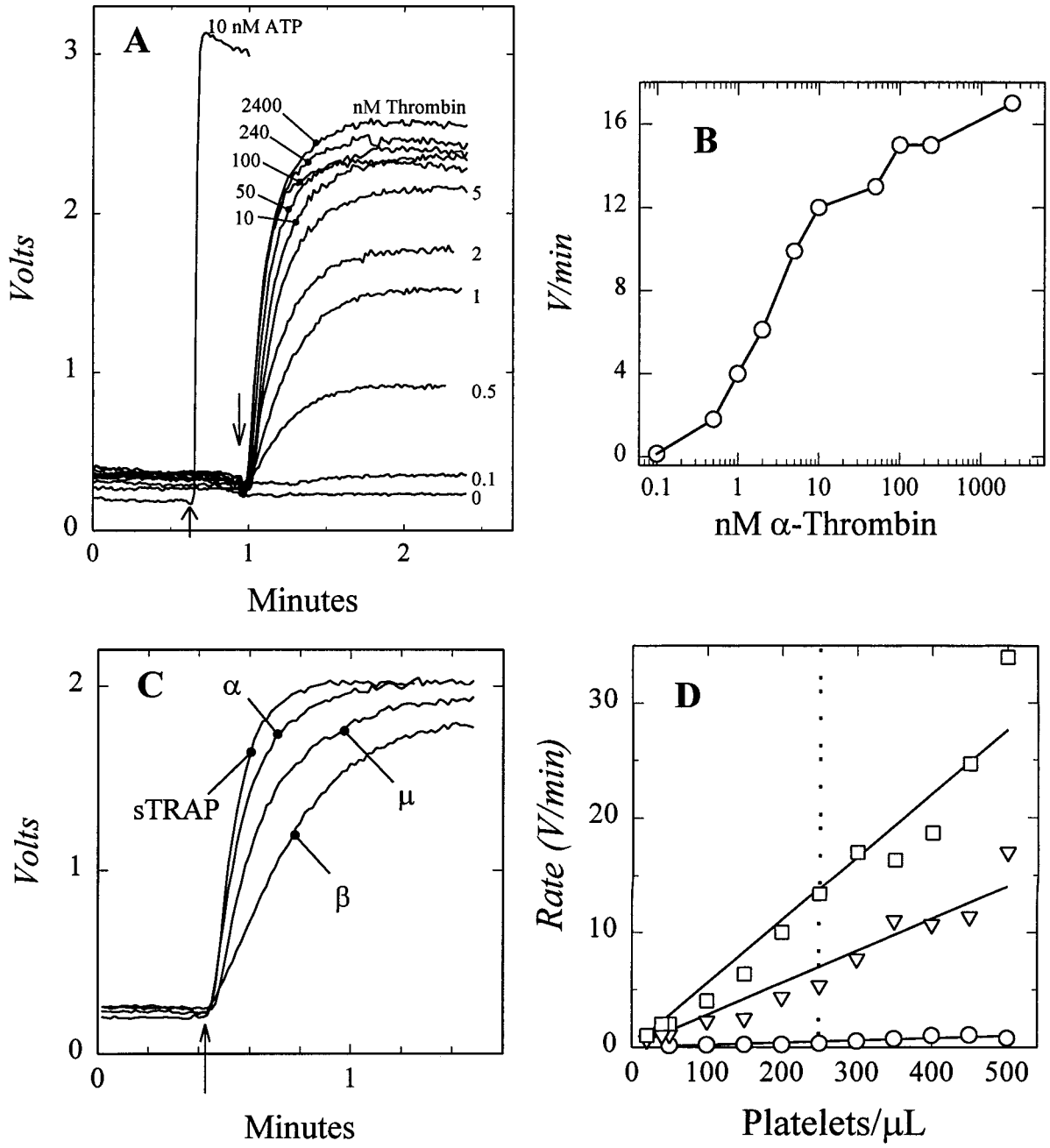

FIGURE 3: Dense body secretion assay. (A) Platelets (250 per μL) were activated by injection of α-thrombin (↓) at the concentrations (final) that are indicated; also shown is a calibrating injection of 10 nM ATP (↑). (B) A plot (data from panel A) of the initial rates of ATP secretion vs thrombin concentration. (C) Progress curves of ATP secretion initiated with 25 nM α-thrombin, 100 nM μ-thrombin, 75 nM β-thrombin, and 5 μM sTRAP. (D) The relationship between platelet concentration and secretion response to 0.1 (○), 1 (▽), and 10 nM (□) α-thrombin; the vertical dotted line denotes the routine platelet concentration.

In contrast, the β-thrombin dose response (Figure 5A, lower group) lies another log unit to the right, more nearly congruent with that of ATP secretion. Also in contrast to ATP secretion, the $Ca(II)_C$ transients stimulated by α-thrombin and μ-thrombin, in concentrations near their thresholds for ATP secretion, are unaffected by preincubation of the platelets with anti-$PAR1_T$ Ig (Figure 5B).

Impact of FPR-α-Thrombin on Responses to Active Enzyme. Enzymatically inactive FPR-thrombin binds nonsubstrate ligands, including hirudin tail and related peptides, and GP Ib, but cannot bind substrates, including $rPAR1_T$ (Figure 2). Addition of FPR-α-thrombin to platelets causes a dose-dependent inhibition of the ATP secretion response to low agonist concentrations of α-thrombin, μ-thrombin, and sTRAP, and to a lesser extent β-thrombin (Figure 6A). This inhibition is partially overcome by increases in the respective agonist concentrations, except for the ≈40% inhibition of the β-thrombin-induced response, which is not alleviated by increased agonist concentration (Figure 6B). Monoclonal Ig LJ-Ib10, directed against the FPR-thrombin-binding site on GP Ib, likewise inhibits the responses to the thrombins with features similar to those with the FPR-α-thrombin, but in contrast has no impact on the response to sTRAP (Figure 6C). This finding implies that FPR-thrombin may have a receptor distinct from GP Ib and $PAR1_T$.

In contrast, the rise in $Ca(II)_C$ in response to concentrations of α-thrombin near the threshold for ATP secretion is minimally affected by FPR-α-thrombin at concentrations that

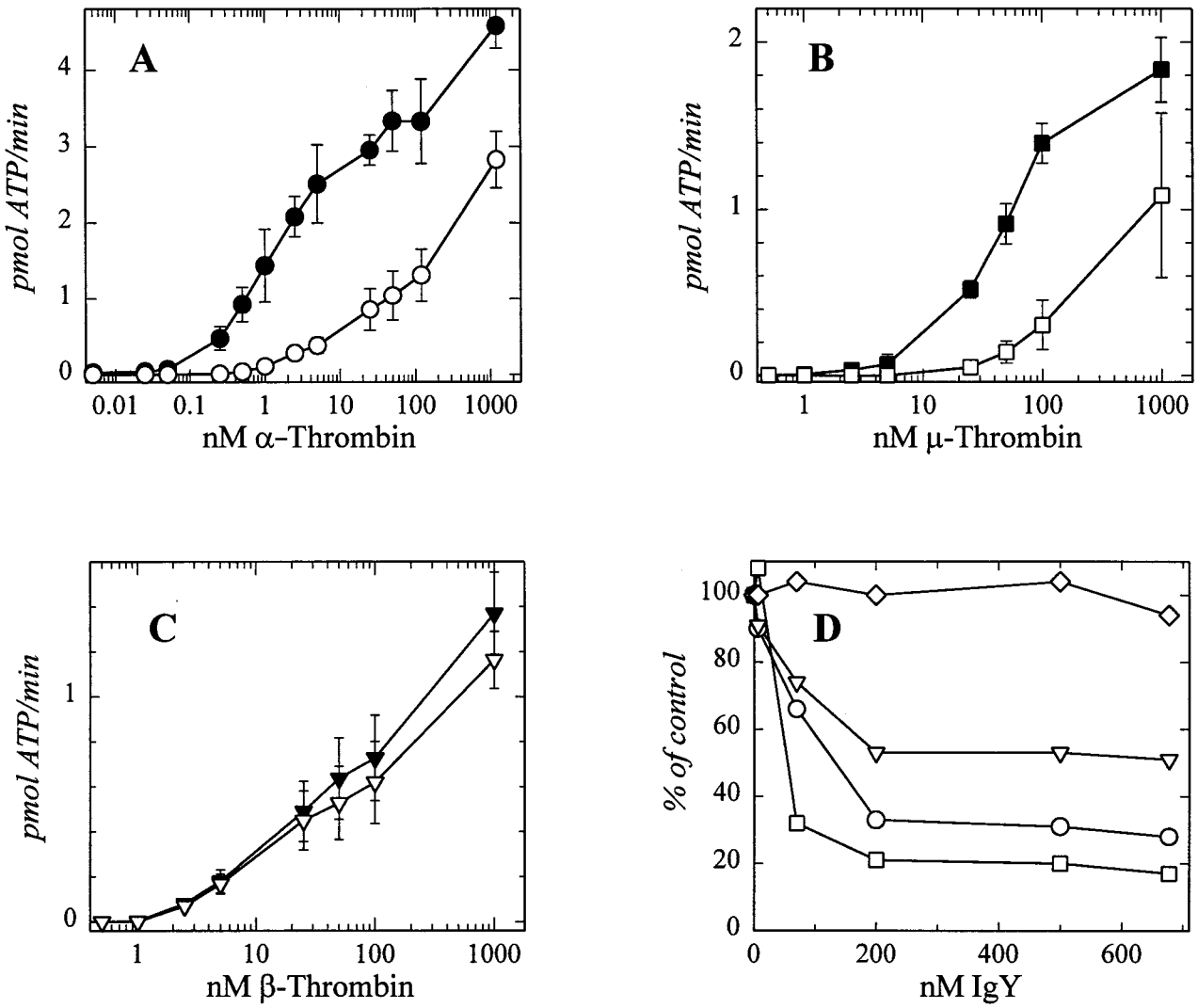

FIGURE 4: Effect of anti-rPAR1$_T$ Ig on platelet ATP secretion in response to thrombin variants and TRAP. Platelets incubated with 70 nM chicken anti-rPART IgY for 20 min before initiating dose responses (white symbols) to α-thrombin (A), μ-thrombin (B), and β-thrombin (C), shown with paired controls (black symbols). Values are presented as the mean ± standard deviation of measurements with three independent platelet preparations. Panel D shows the effect of increasing concentrations of anti-rPAR1$_T$ IgY on the secretion response of platelets stimulated with 25 nM α-thrombin (○), 100 nM μ-thrombin (□), 75 nM β-thrombin (▽), and 5 nM sTRAP (◇). Measurements are presented as a percentage of the response from control (untreated) for each enzyme.

strongly inhibit ATP secretion (Figure 7). The slight but reproducible inhibition of the rate of rise in Ca(II)$_C$ observed at low (100−200 pM) thrombin concentrations is not observed with thrombin above 1 nM.

Platelet Desensitization by Thrombin Variants. Proteolytic activation of a receptor is inherently irreversible, and so should become desensitized by subthreshold proteolysis. The half-time for rPAR1$_T$ hydrolysis by 200 pM μ-thrombin is 5 min. Pretreatment of platelets with 200 pM μ-thrombin, which stimulates neither ATP secretion nor a Ca(II)$_C$ rise, desensitized the platelets by 60−70% within 30 min to itself, α-thrombin, and sTRAP, but less so to β-thrombin (Figure 8A). In contrast, pretreatment of platelets with β-thrombin at a concentration far too low to hydrolyze a significant fraction of PAR1$_T$ yielded uniform desensitization of the platelet ATP secretion response to all three thrombin variants as well as to sTRAP (Figure 8B). Concentrations of α-thrombin as low as 1−10 pM desensitize the response within 10−20 min to itself, μ-thrombin, and sTRAP, but less so to β-thrombin (Figure 8C). The desensitization process, which occurs before 10 pM α-thrombin should cleave more than 1% of rPAR1$_T$, is unaffected by preincubation of the platelets with anti-PAR1$_T$ IgY (Figure 8C, crosshair diamonds).

Lack of Synergy between β-Thrombin and μ-Thrombin. The disparate efficiencies of β- and μ-thrombins in rPAR1$_T$ hydrolysis in the face of more nearly equivalent dose responses and the resistance of the β-thrombin response to anti-rPAR1$_T$ Ig suggest that these two enzymes initiate ATP secretion via different receptors. The nonreciprocal desensitization observed with β- and μ-thrombins, along with the disparities in the impact of FPR-thrombin, points further to metabolically interacting processes. This hypothesis predicts that coactivating platelets with equimolar amounts of β- and μ-thrombins would reconstitute the dose response to α-thrombin. However, these enzymes in either equimolar or equi-EC$_{50}$ concentrations manifested no synergism in platelet ATP secretion (Figure 9).

DISCUSSION

Assay. Platelets offer a network of intracellular and intercellular signaling cascades that serve to obscure stimulus−

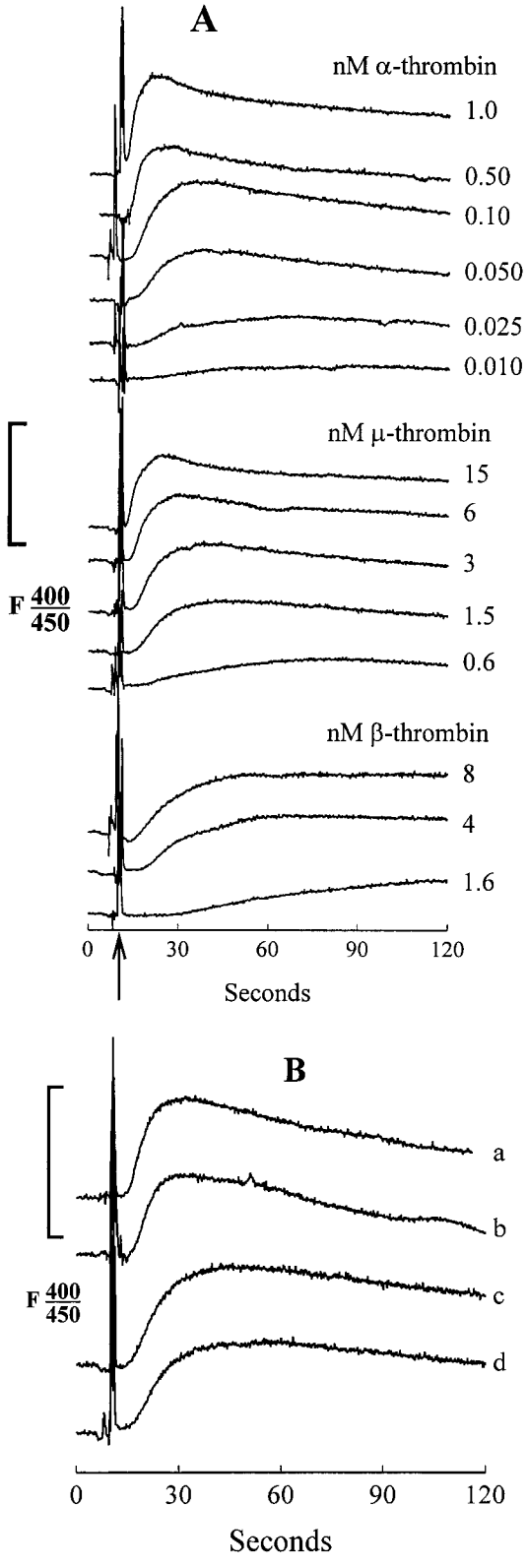

FIGURE 5: Changes in $Ca(II)_C$ in response to thrombin variants. (A) Platelets loaded with indo-1 were stimulated (↑) with α-thrombin, μ-thrombin, and β-thrombin at the indicated concentrations. (B) Platelets loaded with indo-1 were stimulated with 200 pM α-thrombin after incubation (30 min at 30 °C) with 70 nM preimmune IgY (a) or anti-$rPAR1_T$ IgY (b), or with 1.5 nM μ-thrombin after incubation (30 min at 30 °C) with 70 nM preimmune IgY (c) or anti-$rPAR1_T$ IgY (d). The basal fluorescence ratios (400 nm/450 nm) ranged between 1.2 and 1.4; the bracket on the *y*-axis denotes the magnitude of deflection observed when the ratio doubles.

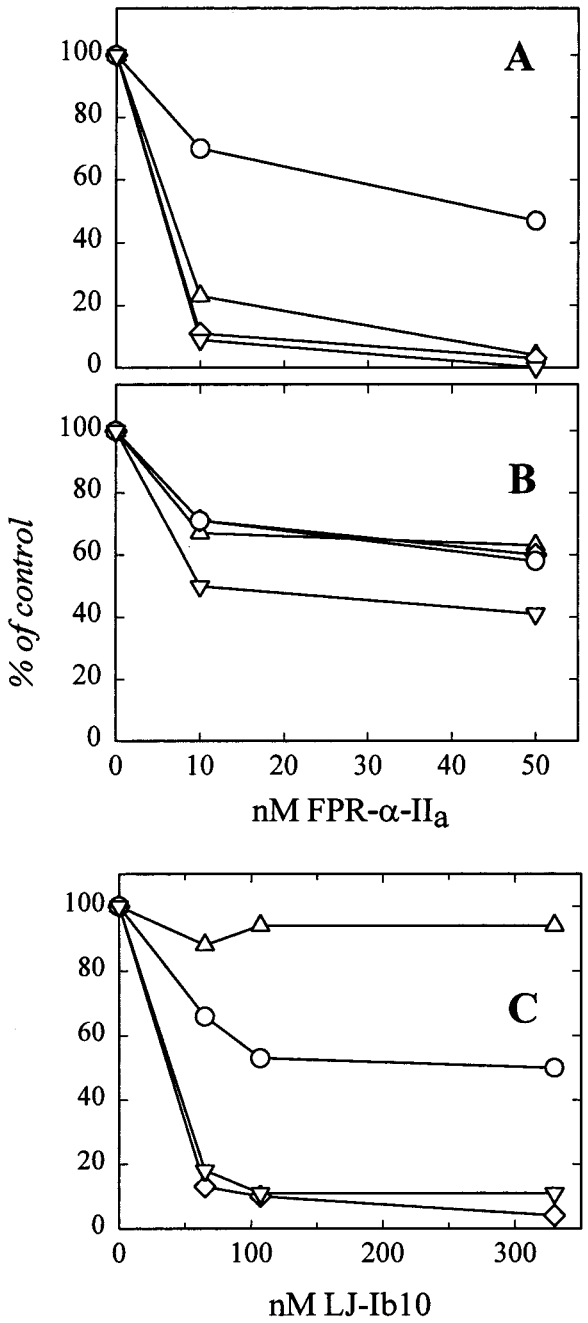

FIGURE 6: Effect of GP Ib ligands FPR-thrombin (A and B) and monoclonal Ig LJ-1B10 (C) on platelet ATP secretion response to α-thrombin (○), μ-thrombin (□), β-thrombin (▽), and sTRAP (◇) in low (A and C) and high (B) concentrations. Low concentrations (A and C) were as follows: 0.5 nM α-thrombin, 10 nM β-thrombin, 10 nM μ-thrombin, and 1 μM sTRAP. High concentrations (B) were as follows: 25 nM α-thrombin, 75 nM β-thrombin, 100 nM μ-thrombin, and 10 μM sTRAP. These measurements were repeated twice as shown and thrice or more with single antagonist concentrations.

response relationships. At physiological platelet densities, paracrine propagation by ADP and thromboxane A2 and by physical association of platelets have led to introduction of reagents such as apyrase and aspirin which enhance the value of primary platelet responses as bases for quantitative assays (*43*). While detailed treatment of methodology lies beyond the intent of this paper, some features of the platelet assays, designed in particular to circumvent the intercellular signals, warrant comment. The use of a firefly-luciferase-coupled ATP secretion assay for the detection of platelet activation

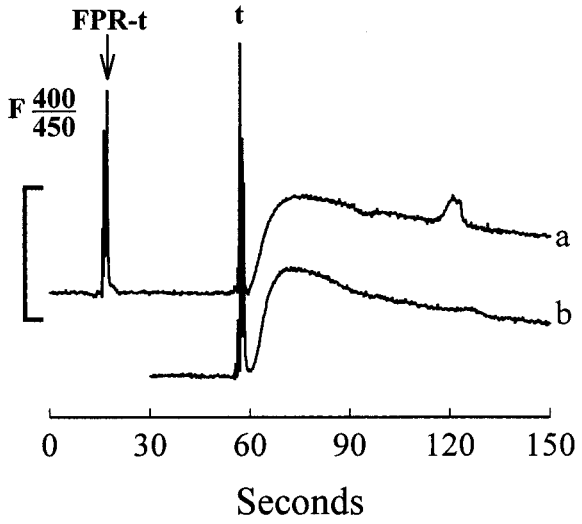

FIGURE 7: Effect of FPR-thrombin on the change in $Ca(II)_C$ in response to α-thrombin. Platelets loaded with indo-1 were incubated (a) with 26 nM FPR-thrombin (added at arrow) and then stimulated with 200 pM α-thrombin (t). The control without FPR-thrombin is trace b. Progress curves are representative of three platelet preparations assayed at low (100−200 pM) α-thrombin concentrations. The bracket on the *y*-axis denotes the magnitude of deflection observed when the ratio doubles.

has been in routine use in the form of platelet lumiaggregometry in which washed platelets or platelet-rich plasma is mixed with a luciferin and luciferase reagent and activation is detected as light output. The typical concentrations at which such assays are performed ($>3 \times 10^8$ mL^{-1}) do not resolve the effects of agonist from those of paracrine cross-talk and physical contact between platelets. A 1000-fold dilution of whole blood (not shown) or platelet-rich plasma in a nutrient medium that provides short-term platelet stability (several hours to days) enables the direct observation of agonist-induced platelet ATP secretion free from the contribution of cooperative paracrine and contact effects (Figure 3), and spares the need for addition of inhibitors of such activities. At the higher platelet concentrations used for measurement of $Ca(II)_C$ (but still 100-fold diluted from plasma), the absence of an impact of collagen on the fluorescence signal likewise implies the absence of paracrine stimulation (*42*). The assay of platelets after direct ultradilution provides the added advantages of extinction of the soluble coagulation factors and inhibitors as well as rapid (30 s) and simple preparation of working platelet suspensions from very small samples (10 μL of blood or PRP yields 10−20 mL of dilute platelets) without intervening anticoagulation or centrifugation. The initial rate of ATP secretion is tightly coupled to the concentration of agonist and yields consistent dose−response curves. Finally, the low platelet concentration ensures that nominal (total) and free thrombin concentrations are equal in all ranges.

Proteolysis and Activation. Long surmised to require catalytically active enzyme (*1*), the mechanism of platelet activation by thrombin has sustained controversy, particularly with respect to the distinction between the occupancy of a receptor and proteolysis of a membrane substrate. While the cloning of $PAR1_T$ (*3*, *4*) established proteolysis as a process in the activation path, the significance of nonproteolytic interactions of thrombin at the platelet membrane remains a subject of debate (*2*, *19*−*28*, *43*), as has the number of

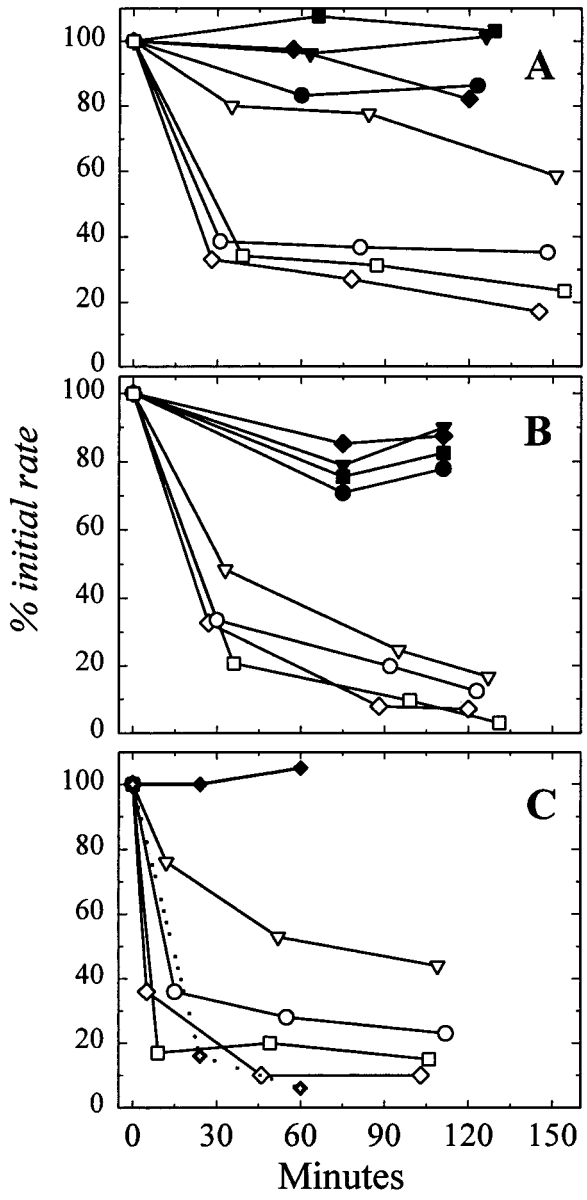

FIGURE 8: Desensitization of platelet ATP secretion response by thrombin variants. Platelets treated with 200 pM μ-thrombin (A), 200 pM β-thrombin (B), or 10 pM α-thrombin (C) were assayed at the times indicated for ATP secretion responses to 25 nM α-thrombin (○), 500 nM μ-thrombin (□), 500 nM β-thrombin (▽), and 5 μM sTRAP peptide (◇). Data for the corresponding untreated controls are represented by black symbols. Data are presented as percentages of the corresponding initial ATP secretion rates for each agonist control measured at the indicated times, and typify one of triplicate experiments. In panel C, the crosshair diamonds (dotted line) show the response to 5 μM sTRAP of platelets incubated (30 min at 30 °C) with 70 nM anti-$PAR1_T$ IgY before addition of the 10 pM α-thrombin; the black diamonds represent data for the corresponding control that shows no effect of the IgY on the response to sTRAP.

distinct PAR_Ts. Indirect evidence for a second PAR_T on human platelets (*8*−*11*) gained credence with the cloning of PAR3 (*15*) and PAR4 (*16*, *17*).

These additional characteristics of platelet responses reflect two, or more, functioning PAR_Ts: (1) disparities in $rPAR1_T$ catalytic efficiencies and secretagogue activities of α-, β-, and μ-thrombins, (2) differential desensitization with β- and μ-thrombins, (3) the disconnected α-thrombin and μ-thrombin dose responses of $Ca(II)_C$ fluxes and ATP secretion, and

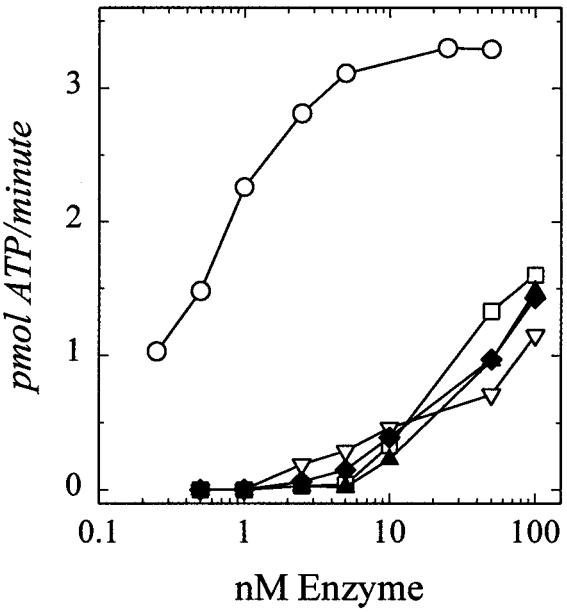

FIGURE 9: Assay for synergism of β-thrombin and μ-thrombin. Secretion of ATP was assayed in response to α-thrombin (○), μ-thrombin (□), β-thrombin (▽), and mixtures of μ-thrombin and β-thrombin in equimolar (◆) and equi-EC_{50} (▲) ratios. Measurements with three individual platelet preparations showed no synergy in the face of a 3-fold variation in the EC_{50} of the α-thrombin dose response.

(4) the sensitivity of neither $Ca(II)_C$ fluxes nor α-thrombin desensitization to anti-$PAR1_T$ Ig or FPR-thrombin. The finding that the $Ca(II)_C$ response is disproportionately sensitive to α-thrombin and is affected by neither FPR-thrombin nor anti-$PAR1_T$ Ig suggests further that more than two receptors and/or substrates may be involved, inasmuch as the β-thrombin pathway is likewise relatively insensitive to specific blockade. It should be noted that the dose response of $Ca(II)_C$, more sensitive to α-thrombin or less sensitive to GP Ib ligands than generally reported (*20*, *25*, *26*, *42*−*46*), was acquired at 22 °C with low platelet concentrations, porcine thrombin, a physiological Ca(II) concentration in the medium, indo-1 as indicator, and other detail differences; analysis of the differences may indeed shed some light on nature of the signaling networks. This system may be complicated further by the finding that the $PAR1_T$ activation peptide, likely too dilute to have an impact in this study, has agonist activity that exceeds that of TRAP1 (*47*).

In any case, it is clear that α-thrombin has a unique, $PAR1_T$-independent activity, not shared by β- and μ-thrombins or inactive α-thrombin, and not blocked by ligation of GP Ib. If this process is likewise proteolytic, thrombin enzymology offers an interesting estimate of kinetics. Limited by turnover number, thrombin catalytic efficiency (k'') has an upper limit of about 10^8 M^{-1} s^{-1} (k'' with $rPAR1_T$ is $^1/_3$ of that). If there were, for the sake of estimation, 2000 copies per platelet of the high-sensitivity receptor for the $Ca(II)_C$ response, then platelets showing a response to 20 pM thrombin within 10 s would be doing so with no more than 20 turnovers ($N = N_0e^{-k't}$), if the interaction were bimolecular.

Asymmetric desensitization of platelets by μ- and β-thrombins provides circumstantial evidence for direct, possibly structural linkage of $PAR1_T$ and a second PAR_T. Rapid desensitization with 200 pM β-thrombin of the secretory response to all thrombins (Figure 8B) corroborates the existence of a relatively sensitive membrane substrate, needed to account for the secretory response to β-thrombin in nanomolar concentrations. Agonist activity (ATP secretion) of β-thrombin is 10% of that of α-thrombin in the face of less than 1% clotting activity, a 2 log unit right shift in the response of $Ca(II)_C$ (Figure 5), and a marked reduction in the affinity of binding of this enzyme to platelets (*48*−*50*). Tracy et al. (*26*−*28*) have found that exosite 1 specificity, lost in β-thrombin, is essential for high-affinity, noncatalytic interaction of thrombin with platelets. These interactions thus appear to attenuate the thrombin response through a yet undefined inhibitory reaction for which elevation of $Ca(II)_C$ is unnecessary; analysis of receptor phosphorylation (*51*) may provide some insight. Likewise, partial inhibition of the secretory response to β-thrombin by both anti-$rPAR1_T$ (Figure 4) and SPAN12 (data not shown), in the face of resistance of $rPAR1_T$ cleavage by β-thrombin, suggests some functional connection of $PAR1_T$ to the process initiated by β-thrombin. Inhibition by FPR-thrombin of the response to sTRAP implies further that occupancy of either glycoprotein Ib/IX or other membrane proteins by α-thrombin uncouples a link between $PAR1_T$ and a second process. Because μ-thrombin, which cleaves $PAR1_T$ efficiently, is not synergistic with respect to β-thrombin, a two-receptor system would require coordinate activation of both receptors to explain the strong agonist activity of α-thrombin. Otherwise, a third receptor might account for the behavior. The nature of a putative link remains unexplored, but glycoprotein Ib is known to be a component of a multisubunit complex of glycoproteins (*52*), and the molecular mass of the thrombin "receptor" has been deduced to be near 10^6 (*53*). Inactive thrombin does not inhibit the thrombin-stimulated secretory response of cultured human endothelium (*54*) which likewise responds via $PAR1_T$ (*55*) and expresses the complete GP Ib−GP V−GP IX complex (*56*).

Glycoprotein Ib, either from direct investigation (*19*, *20*) or as inferred from binding measurements carried out before its associations with thrombin were clarified (*2*), has been characterized as a thrombin receptor that in some fashion participates in platelet activation. Inhibition of sTRAP by FPR-thrombin but not by LJ-Ib10 confirms that, as argued by Jamieson (*57*), some nonproteolytic interaction of thrombin influences $PAR1_T$ function independent of the site of proteolysis. Our findings, therefore, support the hypothesis that the occupancy of glycoprotein Ib by active α-thrombin indirectly attenuates the responses to PAR_T hydrolysis, and possibly accounts for a dose response spanning 6 log units between the $Ca(II)_C$ threshold and the upper end of ATP secretion. The apparent absence of any metabolic signal coupled to thrombin binding and the absence of synergy between β-thrombin and μ-thrombin raise the hypothesis that liganding of glycoprotein Ib or associated proteins can break a linkage in proteolysis of two or more PAR_Ts. The different impacts on the response to sTRAP of FPR-thrombin and antibody LJ-Ib10, imputed to bind to a common site on GP Ib (*20*, *22*, *23*), suggest that the complex may be yet more elaborate than any existing models, if not something completely different.

ACKNOWLEDGMENT

Zaverio Ruggeri (Scripps Institute, La Jolla, CA) provided monoclonal Ig LJ-Ib10. Lawrence F. Brass (University of Pennsylvania, Philadelphia, PA) provided SPAN12. Robert Litwiller (Mayo Foundation) synthesized and HPLC-purified sTRAP. Oligonucleotide primers were synthesized by the Mayo Foundation Molecular Biology Core Facility. The Mayo Foundation Mass Spectrometry Core Facility provided MALDITOF-MS support.

REFERENCES

1. Davey, M. G., and Luscher, E. F. (1967) *Nature 216*, 857−858.
2. Tollefsen, D. M., Feagler, J. R., and Majerus, P. W. (1974) *J. Biol. Chem. 249*, 2646−2651.
3. Rasmussen, U. B., Vouret-Craviari, V., Jallat, S., Schlesinger, Y., Pages, G., Pavirani, A., Lecocq, J. P., Pouyssegur, J., and Van Obberghen-Schilling, E. (1991) *FEBS Lett. 288*, 123−128.
4. Vu, T. K., Hung, D. T., Wheaton, V. I., and Coughlin, S. R. (1991) *Cell 64*, 1057−1068.
5. Bar-Shavit, R., and Wilner, G. D. (1986) *Semin. Thromb. Hemostasis 12*, 244−249.
6. Ozawa, K., Takahashi, M., and Sobue, K. (1996) *FEBS Lett. 382*, 159−163.
7. Crago, A. M., Wu, H. F., Hoffman, M., and Church, F. C. (1995) *Exp. Cell Res. 219*, 650−656.
8. Henriksen, R. A., and Brotherton, A. F. (1983) *J. Biol. Chem. 258*, 13717−13721.
9. McGowan, E. B., and Detwiler, T. C. (1986) *J. Biol. Chem. 261*, 739−746.
10. Henriksen, R. A., Samokhin, G. P., and Tracy, P. B. (1997) *Arterioscler. Thromb. Vasc. Biol. 17*, 3519−3526.
11. Seiler, S. M., Goldenberg, H. J., Michel, I. M., Hunt, J. T., and Zavoico, G. B. (1991) *Biochem. Biophys. Res. Commun. 181*, 636−643.
12. Brass, L. F., Vassallo, R. R., Jr., Belmonte, E., Ahuja, M., Cichowski, K., and Hoxie, J. A. (1992) *J. Biol. Chem. 267*, 13795−13798.
13. Connolly, T. M., Condra, C., Feng, D. M., Cook, J. J., Stranieri, M. T., Reilly, C. F., Nutt, R. F., and Gould, R. J. (1994) *Thromb. Haemostasis 72*, 627−633.
14. Connolly, A. J., Ishihara, H., Kahn, M. L., Farese, R. V., Jr., and Coughlin, S. R. (1996) *Nature 381*, 516−519.
15. Ishihara, H., Connolly, A. J., Zeng, D., Kahn, M. L., Zheng Y. W., Timmons, C., Tram, T., and Coughlin, S. R. (1997) *Nature 386*, 502−506.
16. Xu, W. F., Andersen, H., Whitmore, T. E., Presnell, S. R., Yee, D. P., Ching, A., Gilbert, T., Davie, E. W., and Foster, D. C. (1998) *Proc. Natl. Acad. Sci. U.S.A. 95*, 642−646.
17. Kahn, M. L., Zheng, Y. W., Huang, W., Bigornia, V., Zeng, D., Moff, S., Farese, R. V., Jr., Tam, C., and Coughlin, S. R. (1998) *Nature 394*, 690−694.
18. Ishihara, H., Zeng, D., Connolly, A. J., Tam, C., and Coughlin, S. R. (1998) *Blood 91*, 4152−4157.
19. Harmon, J. T., and Jamieson, G. A. (1986) *J. Biol. Chem. 261*, 13224−13229.
20. De Marco, L., Mazzucato, M., Masotti, A., Fenton, J. W., II, and Ruggeri, Z. M. (1991) *J. Biol. Chem. 266*, 23776−23783.
21. Gralnick, H. R., Williams, S., McKeown, L. P., Hansmann, K., Fenton, J. W., II, and Krutzsch, H. (1994) *Proc. Natl. Acad. Sci. U.S.A. 91*, 6334−6338.
22. Greco, N. J., Tandon, N. N., Jones, G. D., Kornhauser, R., Jackson, B., Yamamoto, N., Tanoue, K., and Jamieson, G. A. (1996) *Biochemistry 35*, 906−914.
23. Harmon, J. T., and Jamieson, G. A. (1986) *J. Biol. Chem. 261*, 15928−15933.
24. Greco, N. J., Tenner, T. E., Jr., Tandon, N. N., and Jamieson, G. A. (1990) *Blood 75*, 1989−1990.
25. De Marco, L., Mazzucato, M., Masotti, A., and Ruggeri, Z. M. (1994) *J. Biol. Chem. 269*, 6478−6484.
26. Leong, L., Henriksen, R. A., Kermode, J. C., Rittenhouse, S. E., and Tracy, P. B. (1992) *Biochemistry 31*, 2567−2576.
27. Hayes, K. L., Leong, L., Henriksen, R. A., Bouchard, B. A., Ouellette, L., Church, W. R., and Tracy, P. B. (1994) *J. Biol. Chem. 269*, 28606−28612.
28. Hayes, K. L., and Tracy, P. B. (1999) *J. Biol. Chem. 274*, 972−980.
29. Bode, W., Turk, D., and Karshikov, A. (1992) *Protein Sci. 1*, 426−471.
30. Vu, T. K., Wheaton, V. I., Hung, D. T., Charo, I., and Coughlin, S. R. (1991) *Nature 353*, 674−677.
31. Owen, W. G., Esmon, C. T., and Jackson, C. M. (1974) *J. Biol. Chem. 249*, 594−605.
32. Lollar, P., Knutson, G. J., and Fass, D. N. (1984) *Blood 63*, 1303−1308.
33. Morita, T., and Iwanaga, S. (1978) *J. Biochem. 83*, 559−570.
34. Braun, P. J., Hofsteenge, J., Chang, J., and Stone, S. R. (1988) *Thromb. Res. 50*, 273−283.
35. Chase, T., Jr., and Shaw, E. (1969) *Biochemistry 8*, 2212−2224.
36. Lundblad, R. L., Nesheim, M. E., Straight, D. L., Sailor, S., Bowie, J., Jenzano, J. W., Roberts, J. D., and Mann, K. G. (1984) *J. Biol. Chem. 259*, 6991−6995.
37. Polson, A., Coetzer, T., Kruger, J., von Maltzahn, E., and van der Merwe, K. J. (1985) *Immunol. Invest. 14*, 323−327.
38. Brass, L. F., Pizarro, S., Ahuja, M., Belmonte, E., Blanchard, N., Stadel, J. M., and Hoxie, J. A. (1994) *J. Biol. Chem. 269*, 2943−2952.
39. Seiler, S. M., Peluso, M., Tuttle, J. G., Pryor, K., Klimas, C., Matsueda, G. R., and Bernatowicz, M. S. (1996) *Mol. Pharmacol. 49*, 190−197.
40. Hill-Eubanks, D. C., and Lollar, P. (1990) *J. Biol. Chem. 265*, 17854−17858.
41. Martinelli, R. A., and Scheraga, H. A. (1980) *Biochemistry 19*, 2343−2350.
42. Packham, M. A., Rand, M. L., Ruben, D. H., and Kinlough-Rathbone, R. L. (1991) *Comp. Biochem. Physiol., A: Physiol. 99*, 551−557.
43. Kinlough-Rathbone, R. L., Perry, D. W., Rand, M. L., and Packham, M. A. (1997) *Thromb. Haemostasis 77*, 741−747.
44. Jamieson, G. A. (1997) Pathophysiology of the thrombin receptor. *Thromb. Haemostasis 78*, 242−246.
45. Heemskerk, J. W., Feijge, M. A., Henneman, L., Rosing, J., and Hemker, H. C. (1997) *Eur. J. Biochem. 249*, 547−555.
46. Jy, W., and Haynes, D. H. (1987) *Biochim. Biophys. Acta 929*, 88−102.
47. Furman, M. I., Liu L., Benoit, S. E., Becker, R. C., Barnard, M. R., and Michelson, A. D. (1998) *Proc. Natl. Acad. Sci. U.S.A. 95*, 3082−3087.
48. Mohammed, S. F., Whitworth, C., Chuang, H. Y., Lundblad, R. L., and Mason, R. G. (1976) *Proc. Natl. Acad. Sci. U.S.A. 73*, 1660−1663.
49. Jandrot-Perrus, M., Huisse, M. G., Krstenansky, J. L., Bezeaud, A., and Guillin, M. C. (1991) *Thromb. Haemostasis 66*, 300−305.
50. Jandrot-Perrus, M., Huisse, M. G., Ternisien, C., Bezeaud, A., and Guillin, M. C. (1992) *Semin. Thromb. Hemostasis 18*, 261−266.
51. Ishii, K., Chen, J., Ishii, M., Koch, W. J., Freedman, N. J., Lefkowitz, R. J., and Coughlin, S. R. (1994) *J. Biol. Chem. 269*, 1125−1130.
52. Ruggeri, Z. M. (1991) *Prog. Hemostasis Thromb. 10*, 35−68.
53. Harmon, J. T., and Jamieson, G. A. (1985) *Biochemistry 24*, 58−64.
54. Lollar, P., and Owen, W. G. (1980) *J. Biol. Chem. 255*, 8031−8034.
55. Bouton, M. C., Jandrot-Perrus, M., Moog, S., Cazenave, J. P., Guillin, M. C., and Lanza, F. (1995) *Biochem. J. 305*, 635−641.

56. Wu, G., Essex, D. W., Meloni, F. J., Takafuta, T., Fujimura, K., Konkle, B. A., and Shapiro, S. S. (1997) *Blood. 90*, 2660−2669.
57. Jamieson, G. A., and Okumura, T. (1978) *J. Clin. Invest. 61*, 861−864.
58. Schagger, H. A., and von Jagow, G. (1987) *Anal. Biochem. 166*, 368−379.

BI9827518